



Published in final edited form as:

Biomed Pharmacother. 2020 November ; 131: 110665. doi:10.1016/j.biopha.2020.110665.

Myosin light chain kinase is a potential target for hypopharyngeal cancer treatment

Feng Cao^{#a,b}, Le Zhu^{#c,d}, Jing Zhang^{c,d}, Pawin Pongkorpsakol^e, Wei-Ting Kuo^f, Jerrold R. Turner^f, Qing Zhou^{c,d}, Yuan Wang^{c,d}, Feihu Chen^g, Yehai Liu^{a,**}, Li Zuo^{c,d,f,*}

^aDepartment of Otorhinolaryngology Head and Neck Surgery, The First Affiliated Hospital of Anhui Medical University, Hefei, 230032, China ^bDepartment of Otorhinolaryngology Head and Neck Surgery, The Second People's Hospital of Hefei, 230001, China ^cLaboratory of Molecular Biology, and Department of Biochemistry, Anhui Medical University, Hefei, Anhui, 230032, China ^dKey Laboratory of Gene Research of Anhui Province, Hefei, Anhui, 230032, China ^eTranslational Medicine Graduate Program, Faculty of Medicine, Ramathibodi Hospital, Mahidol University, Bangkok, Thailand ^fDepartment of Pathology, Brigham and Women's Hospital and Harvard Medical School, United States ^gCollege of Pharmacy, Anhui Medical University, Hefei, China

These authors contributed equally to this work.

Abstract

Hypopharyngeal cancer is squamous cell carcinoma (SCC) with the worst prognosis among the head and neck cancers. Overall, the 5-year survival rate remains poor although diagnostic imaging, radiation, chemotherapy, and surgical techniques have been improved. The mortality of patients with hypopharyngeal cancer is partly due to an increased likelihood of developing a second primary malignancy and metastasis. In this study, we found that MLCK expression, compared to healthy tissue, was up-regulated in hypopharyngeal tumor tissue. Of particular interest, a low 5-year survival rate was positively correlated with MLCK expression. We hypothesized that MLCK might be a target for hypopharyngeal cancer prognosis and treatment. In order to explore the function of MLCK in the development of cancer, we knockdown MLCK in hypopharyngeal cancer FaDu cells. The results showed that MLCK knockdown reduced the migration and invasion of FaDu cells. 4-amino-2-trifluoromethylphenyl retinate (ATPR) is the derivative of all-trans retinoic acid (ATRA), which was able to reduce both MLCK expression and activity in FaDu cells. ATPR induced FaDu cells apoptosis in a dose-dependent manner and also inhibited cell growth both *in vivo* and *in vitro*. Further experiments showed that overexpression of MLCK reduced ATPR induced-migration inhibition while increase of ATPR induced apoptosis, which suggested that MLCK was involved in ATPR's anti-cancer function. In conclusion, MLCK is a novel

This is an open access article under the CC BY-NC-ND license (<http://creativecommons.org/licenses/by-nc-nd/4.0/>).

*Corresponding author at: Laboratory of Molecular Biology, and Department of Biochemistry, Anhui Medical University, Hefei, Anhui, 230032, China. lizuo1981@163.com (L. Zuo). **Corresponding author. liuyehai616@qq.com (Y. Liu).

Author contributions

FC, LZ, and JZ performed the experiments. YHL and LZ designed the study, YHL drafted and wrote the manuscript. PP revised the manuscript. FHC supported the ATPR. The work was done in YW and QZ's lab. QZ and YW guided the experiments. JRT supported the revised process including the cells and antibodies. WTK performed the flow assay and revised the manuscript.

Declaration of Competing Interest

The authors report no declarations of interest.

prognostic marker and therapeutic target for hypopharyngeal cancer. By targeting MLCK, ATPR exhibits its potential application in the treatment of this type of cancer.

Keywords

Hypopharyngeal cancer; MLCK; ATRA; ATPR

1. Introduction

In developing world, the incidence of hypopharyngeal cancer has been increased in both men and women [1,2]. Carcinoma of the hypopharynx has the worst prognosis among of all head and neck subsets. These tumors are frequently found at an advanced stage, often are multifocal, and display early submucosal spread. Less than 20% of patients are diagnosed with localized early-stage disease [3]. The hypopharynx is rich in regional lymphatics, leading to the rapid dissemination of these tumors into the nodal basins of the neck [4]. Even the 5-year survival rate is generally increased after the surgery, metastasis, and relapse are still the problem for hypopharyngeal cancer patients. It is urgent to find a way, which can prevent cancer cell metastasis.

The myosin light chain kinase (MLCK) is a crucial enzyme regulating a series of cytoskeleton regulatory proteins. MLCK has been known as the critical regulator of cancer cell metastasis [5-7]. Zhou et al.[8] showed that non-muscle isoform of myosin light chain kinase (nmMLCK) is critical for the rapid dynamic coordination of a series of cytoskeleton regulatory proteins involved in cancer cell proliferation and migration. In addition, MLCK is centrally involved in driving rearrangement of the cytoskeleton, which regulates vascular endothelial barrier function [9], angiogenesis, endothelial cell apoptosis, and leukocytic diapedesis [10]. MLCK has recently been considered as a novel functional protein in cancer initiation, proliferation, migration, and metastasis [11-13].

Recently, we reported that all-trans retinoic acid (ATRA) inhibited colorectal cancer cell migration by suppressing MLCK expression *via* MAPK signaling pathway [14]. ATRA is an active metabolite of vitamin A belonging to the retinoid family. Retinoids exert potent effects on cell growth, differentiation, and apoptosis *via* stimulating its nuclear receptors and have significant promise for cancer therapy. Differentiation therapy with ATRA has marked a significant advance and become the first choice drug in the treatment of acute promyelocytic leukemia (APL) [15,16]. ATRA is increasingly included in anti-tumor therapeutic schemes for the treatment of various diseases such as Kaposi's sarcoma [17], head and neck squamous cell carcinoma [18], ovarian carcinoma [19], bladder cancer [20], neuroblastoma [21]. Also, it produced anti-angiogenic effects in several systems, inhibiting proliferation in vascular smooth muscle cells (VSMCs) and anti-inflammation in rheumatoid arthritis [22]. Our group has modified the chemical structure of ATRA and synthesized a series of compounds. By screening, we found that 4-amino-2-trifluoromethyl-phenyl retinate (ATPR) had better efficacy and solubility. ATPR has been shown to inhibit tumor proliferation and induce apoptosis in gastric cancer [23] and breast cancer [24]. In addition

to solid tumors, ATPR was effective in the treatment of chronic myeloid leukemia(CML) [25,26].

In this study, we demonstrated that MLCK expression was up-regulated in hypopharyngeal carcinoma tissue compared to the non-lesion area. MLCK expression was associated with a 5-year survival rate. Moreover, ATPR inhibited hypopharyngeal cancer cell proliferation both *in vivo* and *in vitro* via MLCK-independent mechanism. However, ATPR inhibited FaDu cell migration, at least in part, by suppressing MLCK expression and activity. Surprisingly, MLCK overexpression promotes cell apoptosis induced by ATPR.

2. Materials and methods

2.1. Human biopsy

All the tissues from patients were collected during May 2007 to March 2013 from the First Affiliated Hospital of Anhui Medical University, total 108 cases including 104 cases of males and 4 cases of females. All subjects had given written informed consent.

2.2. Animals

Experiments were carried out in 4–6-week-old male BALB/c nude mice according to the guidelines of Anhui Medical University Animals center. Mice were housed with *ad libitum* access to food and water and maintained on a 12 h light/dark cycle. Experimental study groups were randomized. All procedures were carried out to minimize the number of animals used (n = 5 per group) and their suffering.

2.3. Cell line and reagents

FaDu cell was obtained from ATCC. Corning Transwell polycarbonate membrane inserts were from Sigma-Aldrich (Cat No: CLS3421). MLCK antibody was a gift from Professor Jerrold R. Turner in Brigham and Women's Hospital (Yenzyme Rb33), pMLC (3671 s) antibody was from cell signaling. MLC antibody was from Abcam (ab79935). Caspases3 (9662 s), cleavage caspases3 (9664 s), Bcl-xl (2764), Bax (2774s), Rock1 (4035) were from Cell Signaling Technology.

2.4. Immunohistochemical staining

Tissue was cut into 5 μ m sections on clean, charged microscope slides and then heated in a tissue-drying oven for 45 min at 60 °C. Deparaffinization, rehydration and antigen retrieval processes were performed as previously described [27]. In brief, tissue slides were washed by xylene, 100 %, 95 % ethanol, 70 % ethanol, 50 % ethanol, and steamed in 0.01 M sodium citrate buffer, pH 6.0, at room temp for 20 min. All slides were then rinsed in 1x TBS with tween (TBST) and blocked in blocking buffer for 20 min. The slides were incubated with primary antibodies overnight. Slides were washed 3 times with TBST, incubated with biotinylated secondary antibody for 1 h at room temperature, and rinsed with TBST. Alkaline phosphatase streptavidin was applied to slides, incubated at room temperature for 30 min., and slides were rinsed in TBST 3 times, 10 min each. Alkaline phosphatase chromogen substrate was added into each slide. Slides were washed with distilled water.

Finally, Slides were also subsequently dehydrated and mounted as well as the signal of target protein staining was detected.

2.5. Construction and transfection

Briefly, pMagi-GFP and pMagi-IRES-GFP vectors were digested and connected with oligo DNA or target gene, as shown in Table 1. Recombinant lentiviral vectors were produced by transfected 293 T cells (This vector was made by MAGI-LAB company, China). At 70–80 % of cell confluency in a 150-mm cell culture plate, transfection of 293 T cells with appreciate plasmids (pMagi-GFP, pMagi-IRES-GFP, pVSV-G, pMD2.G, or REV) was performed in Opti-MEM (Gibco, USA) according to Lipofectamine™ 3000 kit protocol as previously described [28]. After 6 h of culture in Opti-MEM with transfection reagents, the transfection medium was exchanged with completed DMEM media (10%FBS) (Gibco, USA). Infectious lentiviruses were harvested at 48 h post-transfection and then concentrated. The infectious efficiency was determined by GFP expression. FaDu cells were cultured at a density of 1×10^6 cells per well in 6-well tissue culture plates with DMEM (low glucose) containing 4% FBS. After 16 h, the cells were infected with newly recombined lentiviruses or negative control. Polybrene (8 ng/mL) was added to each well. After 6 h of culture, the culture medium was exchanged with fresh DMEM. The cell photographs were taken under fluorescence microscopes. In addition, real-time PCR (Forward primer : GCTGCCTGACCACGAATATAAG; Reverse: GACACCATCCACTTCATCCTTC) was also used to identify the expression of MLCK mRNA in transfected cells.

2.6. Flow cytometry

For apoptosis detection, cells were seeded (1×10^6 cells) in a T75 culture flask (in triplicate for experiments), and three T75 culture flasks for control (unstained, Annexin only, and propidium iodide only). After 48 h incubation, supernatant (floating apoptotic cells) was collected, and adherent cells ($\sim 2 \times 10^6$ cells) from each T75 flask were trypsinized. The collected cells were washed twice with cold PBS and centrifuged ($1000 \times g$, 5 min, RT). Cell pellet ($\sim 2 \times 10^6$ cells) was resuspended in 400 μ L PBS. Then, cells were stained by combined Annexin V (1 mg/mL) with propidium iodide (PI; 1 mg/mL). For experimental control, cells were unstained and stained with either Annexin V or propidium iodide. Flow cytometry was used to analyze apoptosis in this experiment. Indeed, Annexin V⁻/PI⁻ cells are considered as non-apoptotic cells, whereas Annexin V⁺/PI⁻ and Annexin V⁺/PI⁺ cells are defined as apoptotic and necrotic cells, respectively [29].

For proliferation detection, FaDu cells were trypsinized, centrifuged, and washed twice with cold PBS and resuspended in 100 μ L of a reaction mixture containing Annexin V-FITC and PI, the next step following the manufacturer's instructions (Coulter DNA Prep Reagents Kit, Beckman-Coulter). In all groups, fluorescence was determined from the combined collection of floating and attached cells using flow cytometry, as previously described. The data was analyzed by Flowjo software.

2.7. Wound healing assay

Wound healing assay was performed to determine the cell migration ability of FaDu cells [28]. WT and MLCK knockdown FaDu cells were seeded into 24-well plates and grown

until 80–90 % confluence. Sterilized 10- μ l pipette tip was used to generate cross wounding across the cell monolayer. The debris was washed with PBS three times to remove the floating cells. The migration distance of cells into the wound area was then measured at 48 h. Cells migrated into the wounded area from the border of the wound were photographed under the inverted microscope. A total of nine areas were selected randomly in each well by a 100 \times magnification. The data were analyzed using Quantity One software.

2.8. Migration assay

FaDu cells were trypsinized and resuspended in DMEM with 10 % FBS and counted. FaDu cells at 1×10^5 cells were gently added to the upper compartment of the transwell compartments, 24-well format, with 8 μ m pore size insert. DMEM (2.6 mL) containing 0.5 % FBS and 40 μ g/mL collagen was added to the lower compartment. The transwell inserts were placed to the well by merging the bottom of the insert into the medium. The cells were incubated in the transwell plate at 37 °C and 5% CO₂ for 2.5 h. After 2.5 h, the insert was carefully taken out. Cells that do not migrate through the pores and therefore remain on the upper side of the filter membrane and cell debris need to be gently removed with a cotton swab. The cells on the lower side of the insert filter were fixed quickly with 5% glutaraldehyde for 10 min and stained with 1% crystal violet in 2% ethanol for 20 min. Excess crystal violet was removed by quickly merging the insert in ddH₂O for three to four seconds. Number of cells on the lower side of the filter was counted under a microscope.

2.9. Terminal deoxynucleotidyl transferase dUTP nick end labeling (TUNEL) assay

TUNEL assay was used to detect apoptotic cells, as previously described [30]. In brief, the cells were washed three times in PBS and adjusted to 2×10^7 cells/mL. Cell suspension at 100 μ l/well was seeded into 0.4 μ m transwells (Corning Cat No:3413). Cells were fixed in 1% PFA for 30 min., permeabilized in freshly prepared solution (0.1 % Triton X-100 in 0.1 % sodium citrate, sodium citrate was used for antigen retrieval) for 2 min on ice. The cells were further labeled by TUNEL reaction mixture and incubated for 60 min at 37 °C in a dark humidified atmosphere. Samples were imaged under fluorescence microscopy. For evaluation by fluorescence microscopy, excitation wavelength in the range of 520–560 nm (maximum 540 nm; green) and emission wavelength in the range of 570–620 nm (maximum 580 nm, red) were used for this detection.

2.10. ApopTag® ISOL dual fluorescence apoptosis assay

FaDu cells were fixed in 1% paraformaldehyde/PBS, pH 7.4, preferably for 10 min at room temperature. Fixed FaDu cells were washed twice by PBS, 5 min each. Excess liquid was gently removed. Equilibration buffer (75 μ l) was immediately applied directly to the cells and incubated for at least 10 s at room temperature. Fixed cells were incubated with Strenght TdT Enzyme (55 μ l) in a humidified chamber at 37 °C for 1 h. Furthermore, cells were subsequently placed in Stop/Wash Buffer with shaking for 15 s and incubated for 10 min. After that, specimens were incubated in working strength anti-digoxigenin conjugate and washed three times with PBS for 1 min each. Warmed (room temp.) working strength anti-digoxigenin conjugate (rhodamine) was applied to the slide, and slides were incubated for 30 min at room temperature. From this step, all slides should be protected from the light. Counterstain and mounting after Rhodamine staining were operated.

2.11. Nude mice

FaDu cells (1×10^7 cells/100 μ L) were injected into 4-week old mice. After one week, 30 mice that had generated the xenograft successfully were selected and divided into six groups, including the vehicle control group (DMSO in 0.2 mL PBS/day), and the ATPR group. ATPR was gavaged into mice 10–80 mg/kg daily. Tumor sizes were measured weekly using a venire caliper for the next four weeks.

2.12. Transfection

To generate inducible MLCK-eGFP over-expression cells, FaDu cells were seeded into 100 mm dish (Corning, CLS430167). At 50–70 % confluence, cells were then co-transfected with pSPB-transposase and pPBH-TREtight-MLCK-eGFP. These plasmids were the gifts from professor Jerrold R. Turner, Brigham and Women's Hospital, Harvard Medical School (Boston, MA, USA). Transfection was performed according to Lipofectamine™ 3000 reagent protocol (Thermo Fisher Scientific). Briefly, transfection reagent contains 30 μ g of both DNA plasmids mixed with Opti-MEM media and P3000 reagent. Cells were incubated with transfection reagents. At 12 h post-transfection, cells were then cultured in complete media. The expression of MLCK-eGFP can be induced by treatment with doxycycline (dox). Transfection efficiency was evaluated by eGFP signals.

3. Results

3.1. MLCK expression is elevated in hypopharyngeal carcinoma tissue

To determine the relationship between MLCK expression and hypopharyngeal cancer, we performed immunochemistry in human hypopharyngeal cancer biopsy from 108 patients. Of note, hypopharyngeal cancer is mostly diagnosed in men who smoke tobacco and consume excessive alcohol and uncommon in women. Therefore, we only collected 4 females out of 108 cases. As described previously [31-35], increased Cox-2, and decreased E-cadherin expression were reported in hypopharyngeal cancer. We characterized cancer tissue by two markers mentioned above. Consistent with previous reports, immunochemical assay demonstrated that Cox-2 and E-cadherin expression were increased and decreased in hypopharyngeal cancer tissues, respectively (Fig. 1A, B). Since our previous data showed that MLCK contributed to cancer cell migration, we therefore hypothesized that MLCK might also relate to the severity of this hypopharyngeal cancer. The IHC-stained sections were reviewed and scored independently by two experienced pathologists. Indeed, clinical status of the patients have been blinded to prevent diagnostic bias, and both pathologists had similar accuracy rates. Expression levels of MLCK in tissues were evaluated using the –, \pm , +, ++, +++ scoring system. Sections with 0 %–10 % stained cells were designated as no expression or low expression of MLCK (score of –, \pm); sections with 11–40% stained cells were designated as moderate expression of MLCK (score of +); sections with 41–70% stained cells were designated as strong expression of MLCK (score of ++); sections with 71–100% stained cells were designated as very strong expression of MLCK (score of +++). Interestingly, we found that MLCK was obviously upregulated in the hypopharyngeal cancer tissue compared with the adjacent healthy tissue (Fig. 1C). Indeed, we evaluated MLCK expression into two levels, low (– to \pm) and high (+ to +++). The tissue with less than 10% positive cells was evaluated as low expression, more than 10% positive cells was defined as

high expression. MLCK expression was strongly related to the cancer stage ($P < 0.05$) (Table 2). Of particular importance, MLCK expression is correlated with 5 year survival rate (Fig. 1D). The 5-year survival rate of patients with low MLCK expression was around 68%. On the other hand, the patients with higher MLCK expression, 5 year survival rate was ~ 20%, as shown in Fig. 1D.

3.2. MLCK knockdown reduces cancer cell migration and invasion

In order to evaluate the function of MLCK in hypopharyngeal cancer, FaDu cell line was used as a representative *in vitro* model of this type of cancer. A shRNA against MLCK was used to suppress MLCK expression in FaDu cells. As shown in Fig. 2A, GFP signal was detected in shRNA-MLCK transfected FaDu cells, but not in wild type FaDu cells, indicating successful transfection. In addition, we found that MLCK mRNA was significantly attenuated in shRNA-MLCK transfected cells (~ 70 %). To further explore the effects of MLCK knockdown in cell migration, wound healing assay and transwell migration experiments were performed. The results showed that the migration ability was significantly decreased to 30–40 % in MLCK knockdown FaDu cells, as showed in Fig. 2C-F.

3.3. ATPR inhibits cancer cell migration and invasion via suppressing MLCK signal pathway

Since the data in MLCK knockdown FaDu cells indicates that MLCK mediates migration, we next assessed whether MLCK could be a target for cancer treatment. Therefore, we tested the drug, which can block the MLCK function. The data we published in 2016 showed that ATRA inhibits MLCK expression *via* the MAPK signaling pathway in colorectal cancer cells [14]. However, ATRA has several side effects. In order to overcome this problem, our group synthesized its derivatives based on ATRA structure, called ATPR, which had fewer side effects than ATRA [36]. Here, we found that ATPR significantly decreased MLCK expression in FaDu cells in a dose-dependent manner (Fig 3A, B). In addition to MLCK expression, the effect of ATPR on MLCK activity was investigated. Indeed, we found that ATPR suppressed MLC phosphorylation in FaDu cells (Fig. 3C, D). Because MLC phosphorylation can also be regulated by other kinases, including ROCK and ZIPK, we therefore further investigated the effect of ATPR on the expression of these proteins. Western blot analyses revealed that ATPR had no impact on ROCK expression, but significantly increased ZIPK expression (Fig 3E, F). Of particular interest, we showed that migration rate of FaDu cells treated with various concentrations of ATPR was predominantly decreased compared to the vehicle control (Fig 3G, H). Interestingly, using wound healing assay, we found that ATPR significantly reduced the rate of wound healing in a dose-dependent manner in FaDu cells (Fig. 3I, J). These results indicated that ATPR might be a drug candidate for metastasis in hypopharyngeal cancer, at least in part, by inhibiting the migration process.

3.4. ATPR inhibits cancer cell proliferation in vivo and in vitro

We also demonstrated the effects of ATPR both *in vivo* and *in vitro* models, the FaDu cells were subcutaneously injected into mice, ATPR was administered to mice by daily gavage. Hematoxylin and eosin staining on the heart, liver, spleen, lung, and kidney were performed to test whether ATPR produces toxic effects *in vivo*. Of note, there was no difference in

tissue histopathology between vehicle control and ATPR-treated group, suggesting that ATPR had no significant toxic effects on the mice at least with this dose (Fig. 4A). Impressively, ATPR reduced cancer cell growth in nude mice, as shown in Fig. 4B and C. However, we did not see the tumor metastasis in these mice to evaluate the effects of ATRA on cancer cell migration *in vivo*. Nevertheless, the results showed that ATPR inhibited cancer cell proliferation *in vivo*. Meantime, we examined the effect of ATPR in FaDu cell proliferation using the flow cytometry. The results indicated that ATPR blocked cell proliferation at G0/G1 phase of the cell cycle. The cell population of G0/G1 in the vehicle control cells was around 30–40% and was increased to 60–70% after ATPR treatment (Fig. 4D, E).

3.5. ATPR induces cancer cell apoptosis in FaDu cells

To investigate whether ATPR induces FaDu cell apoptosis, different approaches, including TUNEL, ISOL, and flow cytometry, were performed. The TUNEL staining positive cells were shown as magenta. Apoptotic cells were counted and quantified. ATPR did not influence apoptosis at the concentration of <10 μM , while the apoptosis cells were detected from 20 μM (Fig. 5A, B). Using ISOL staining, we found similar results with TUNEL (Fig. 5C, D). Furthermore, the flow cytometry also showed that apoptosis was detected at 40 μM of ATPR treatment; the apoptotic cell population was over 70% of total FaDu cells (Fig. 5E, F). Moreover, western blot analyses indicated that ATPR increased expression of pro-apoptotic proteins, including cleaved caspase-3 and Bax. On the other hand, ATPR decreased the expression of anti-apoptotic protein such as Bcl-xl (Fig. 5G).

3.6. Effects of MLCK overexpression on anti-cancer activities of ATPR

As shown previously, ATPR is non-toxic and effective for suppressing cell migration, inhibiting proliferation, and inducing apoptosis in hypopharyngeal cancer. Since ATPR inhibited MLCK expression and its activity, we further scrutinize whether ATPR produced anti-cancer effects in hypopharyngeal cancer *via* MLCK-associated mechanism. Inducible pPBH- MLCK-overexpressing FaDu cells were used. Doxycycline (dox) was used to induce MLCK expression in FaDu cells. EGFP signal was detected in dox-treated group which indicates MLCK overexpression in transfected FaDu cells (Fig 6A). By using wound healing assay, the rate of migration was accelerated in dox-treated MLCK-overexpressing FaDu cells (Fig. 6B, C). As expected, ATPR could suppress wound healing in transfected FaDu cells without dox treatment. Interestingly, MLCK overexpression reduced ATPR induced migration inhibition (Fig. 6D, E). This indicates that ATPR-inhibited hypopharyngeal cancer cell migration was in the MLCK-associated manner. In addition, we further investigated the effect of ATPR on proliferation of FaDu cells. Flow cytometry demonstrated that ATPR induced similar G0/G1 arrest in both control and dox-treated MLCK-overexpressing FaDu cells (Fig. 6F, G), suggesting anti-proliferative effect of ATPR was MLCK-independent. Surprisingly, in dox-treated MLCK-overexpressing FaDu cells, pro-apoptotic effect was potentiated compared to the same dose of ATPR treated group (Fig. 6H, I).

4. Discussion

Treatment of patients with hypopharyngeal cancer is currently painful due to poor prognosis. In general, patients with hypopharyngeal cancer have always been diagnosed at late stage. Therefore, it is necessary to find new markers and strategies to provide early detection and treat the patient. Here, we reported that MLCK was obviously up-regulated in human hypopharyngeal cancer tissue compared to normal adjacent tissue. Our results also showed that MLCK is associated with 5-year survival rate. The patient with higher MLCK expression had a lower survival rate. In FaDu cells, MLCK is associated with cell migration and invasion. These data strongly support that MLCK may be a potential marker and therapeutic target for hypopharyngeal cancer.

MLCK protein is encoded by MYLK gene, a single-copy gene located on chromosome 3qcen-q21 [37] that contains two promoters for transcription of smMLCK (5.8 kb) and non-muscle long MLCK (8.1 kb) mRNAs [38]. MLCK is a Ca^{2+} /CaM-dependent enzyme that is responsible for smooth muscle contraction *via* phosphorylation of Ser 19 on MLC, an event that facilitates myosin interaction with actin filaments [39]. The involvement of MLCK in non-muscle cell contraction is not well understood. However, activity of this kinase is associated with force development that results in endothelial cell and epithelial cells tight junction disruption. Long MLCK is a central regulator in immune-mediated barrier loss [40-42]. It also affects cell division and proliferation [43] and cell shape [44,45].

Previous reports showed that during cell migration, myosin II-mediated actomyosin contraction is believed to be required for force generation, which is very important for cell movement. Myosin II may also play a role in membrane protrusion at the leading edge. Since myosin II activity is regulated by MLCK, MLCK is therefore believed to be essential for the force generation necessary for cell migration [6]. Our previous data also demonstrated that MLCK was related to migration process in colorectal cancer cells [28]. Consistent with our findings, we found that knockdown of MLCK in FaDu cells reduced the migration. Therefore, inhibition of MLCK expression might also be a therapeutic strategy for the treatment of hypopharyngeal cancer.

Our previous data showed that ATRA, a vitamin A derivative, inhibited migration of colorectal cells by suppressing MLCK expression *via* MAPK signaling pathway. ATRA is typically a part of anti-cancer regime for APL, along with chemotherapy. However, chronic use of ATRA resulted in many adverse effects including headache, fever, dry skin and mouth, skin rash, swollen feet, sores in the mouth or throat, itching, irritated eyes, and hyperlipidemia. In order to reduce these toxicities and increase its efficiency, our group modified the chemical structure of this compound. Among many different compounds, we found that ATPR had more anti-cancer activity and lower toxicity. Of note, we previously showed that ATPR inhibited proliferation, invasion, and migration of breast cancer cells by independently regulating CRABP2 and FABP5 [46]. ATPR induced cell differentiation in K562 cells by inhibiting eIF3a [26]. Over-expression of eIF3a promoted not only protein expression of c-myc and cyclin D1, but also prevented the expression of p-Raf-1, p-ERK and the myeloid differentiation markers CD11b and CD14 and had an influence on inducing the morphologic mature. Here, we reported that ATPR also decreased MLCK expression and

MLC phosphorylation, which resulted in inhibition of migration in FaDu cells. Of note, apart from MLCK, there are other kinases, i.e. ZIPK, that regulate MLC phosphorylation [47]. Therefore, we also tested the effect of ATPR on ZIPK expression. Unexpectedly, ATPR increased ZIPK expression suggesting that although ZIPK acts as one of the critical regulators of MLC phosphorylation, ZIPK may not be compartmentalized with and not involved in regulation of MLC phosphorylation in this cell type. In nude mice, ATPR inhibited tumor growth in mice injected with FaDu cells. *in vitro*, ATPR inhibited FaDu cell proliferation by inducing G0/G1 arrest. The results also showed that ATPR induced cell apoptosis.

Next, we generated doxycycline-inducible MLCK-overexpressing FaDu cells. ATPR inhibited cell migration was more significant in untreated cells than in dox-treated MLCK-overexpressing FaDu cells. In addition, ATPR similarly induced cell cycle arrest in both dox-treated and untreated, inducible MLCK-overexpressing cells. These data demonstrated that anti-migration and anti-proliferative effects of ATPR were *via* MLCK-associated and independent mechanisms, respectively. Therefore, mechanisms underlying anti-proliferative effect of ATPR need to be investigated in future work. Unexpectedly, pro-apoptotic effect of ATPR was enhanced in dox-treated inducible MLCK-overexpressing FaDu cells. Consistent with previous report, up-regulation of MLCK is associated with apoptosis in immune-mediated colitis [48]. Indeed, the level of MLCK expression may result in different effects on apoptosis, and it will be the next study of this project.

5. Conclusion

Our study demonstrates that MLCK might be a potential target for hypopharyngeal cancer. Also, ATPR might be a drug candidate for hypopharyngeal cancer treatment, which can be combined with other drugs. However, more insights related to mechanisms of drug action and safety profiles need to be further elucidated.

Acknowledgments

We appreciate that professor Jerrold R. Turner for his strong support for this work. We also thank Sheng Quan Zhang for sharing cell culture room with us, and Zhengsheng Wu for evaluating the human biopsy slides.

Funding

This work was supported by National Natural Science Foundation of China grant 81800464 (LZ) and Guanghua grant of the Second Hospital (2014-69), grant of the Second Hospital (2016-23, 2017-47).

References

- [1]. Barul C, Matrat M, Auguste A, Dugas J, Radoi L, Menvielle G, Fevotte J, Guizard AV, Stucker I, Luce D, I.s. group, Welding and the risk of head and neck cancer: the ICARE study, *Occup. Environ. Med* 77 (5) (2020) 293–300, 10.1136/oemed-2019-106080. [PubMed: 31959638]
- [2]. Bradley PJ, Epidemiology of hypopharyngeal cancer, *Adv. Otorhinolaryngol* 83 (2019) 1–14, 10.1159/000492299. [PubMed: 30943510]
- [3]. Eckel HE, Bradley PJ, Natural history of treated and untreated hypopharyngeal cancer, *Adv. Otorhinolaryngol* 83 (2019) 27–34, 10.1159/000492305. [PubMed: 30943503]

- [4]. Koo BS, Lim YC, Lee JS, Kim YH, Kim SH, Choi EC, Management of contralateral N0 neck in pyriform sinus carcinoma, *Laryngoscope* 116 (7) (2006) 1268–1272, 10.1097/01.mlg.0000225936.88411.71. [PubMed: 16826073]
- [5]. Kim DY, Helfman DM, Loss of MLCK leads to disruption of cell-cell adhesion and invasive behavior of breast epithelial cells via increased expression of EGFR and ERK/JNK signaling, *Oncogene* 35 (34) (2016) 4495–4508, 10.1038/onc.2015.508. [PubMed: 26876209]
- [6]. Chen C, Tao T, Wen C, He WQ, Qiao YN, Gao YQ, Chen X, Wang P, Chen CP, Zhao W, Chen HQ, Ye AP, Peng YJ, Zhu MS, Myosin light chain kinase (MLCK) regulates cell migration in a myosin regulatory light chain phosphorylation-independent mechanism, *J. Biol. Chem* 289 (41) (2014) 28478–28488, 10.1074/jbc.M114.567446. [PubMed: 25122766]
- [7]. Kassianidou E, Hughes JH, Kumar S, Activation of ROCK and MLCK tunes regional stress fiber formation and mechanics via preferential myosin light chain phosphorylation, *Mol. Biol. Cell* 28 (26) (2017) 3832–3843, 10.1091/mbc.E17-06-0401. [PubMed: 29046396]
- [8]. Zhou T, Wang T, Garcia JG, Genes influenced by the non-muscle isoform of Myosin light chain kinase impact human cancer prognosis, *PLoS One* 9 (4) (2014), e94325, 10.1371/journal.pone.0094325. [PubMed: 24714365]
- [9]. Zuo L, Kuo WT, Turner JR, Tight junctions as targets and effectors of mucosal immune homeostasis, *Cell. Mol. Gastroenterol. Hepatol* (2020), 10.1016/j.jcmgh.2020.04.001.
- [10]. Dudek SM, Garcia JG, Cytoskeletal regulation of pulmonary vascular permeability, *J. Appl. Physiol* 91 (4) (1985) 1487–1500, 10.1152/jappl.2001.91.4.1487, 2001.
- [11]. Barkan D, Kleinman H, Simmons JL, Asmussen H, Kamaraju AK, Hoenorhoff MJ, Liu ZY, Costes SV, Cho EH, Lockett S, Khanna C, Chambers AF, Green JE, Inhibition of metastatic outgrowth from single dormant tumor cells by targeting the cytoskeleton, *Cancer Res.* 68 (15) (2008) 6241–6250, 10.1158/0008-5472.CAN-07-6849. [PubMed: 18676848]
- [12]. Masur K, Vetter C, Hinz A, Tomas N, Henrich H, Niggemann B, Zanker KS, Diabetogenic glucose and insulin concentrations modulate transcriptome and protein levels involved in tumour cell migration, adhesion and proliferation, *Br. J. Cancer* 104 (2) (2011) 345–352, 10.1038/sj.bjc.6606050. [PubMed: 21179032]
- [13]. Zhou X, Liu Y, You J, Zhang H, Zhang X, Ye L, Myosin light-chain kinase contributes to the proliferation and migration of breast cancer cells through crosstalk with activated ERK1/2, *Cancer Lett.* 270 (2) (2008) 312–327, 10.1016/j.canlet.2008.05.028. [PubMed: 18710790]
- [14]. Zuo L, Yang X, Lu M, Hu R, Zhu H, Zhang S, Zhou Q, Chen F, Gui S, Wang Y, All-trans retinoic acid inhibits human colorectal cancer cells RKO migration via downregulating myosin light chain kinase expression through MAPK signaling pathway, *Nutr. Cancer* 68 (7) (2016) 1225–1233, 10.1080/01635581.2016.1216138. [PubMed: 27564600]
- [15]. Guruvayoorappan Siddikuzzaman C, Berlin Grace VM, All trans retinoic acid and cancer, *Immunopharmacol. Immunotoxicol* 33 (2) (2011) 241–249, 10.3109/08923973.2010.521507. [PubMed: 20929432]
- [16]. Kayser S, Schlenk RF, Platzbecker U, Management of patients with acute promyelocytic leukemia, *Leukemia* 32 (6) (2018) 1277–1294, 10.1038/S41375-018-0139-4. [PubMed: 29743722]
- [17]. Bailey J, Pluda JM, Foli A, Saville MW, Bauza S, Adamson PC, Murphy RF, Cohen RB, Broder S, Yarchoan R, Phase I/II study of intermittent all-transretinoic acid, alone and in combination with interferon alfa-2a, in patients with epidemic Kaposi's sarcoma, *J. Clin. Oncol* 13 (8) (1995) 1966–1974, 10.1200/JCO.1995.13.8.1966. [PubMed: 7636537]
- [18]. Satake K, Takagi E, Ishii A, Kato Y, Imagawa Y, Kimura Y, Tsukuda M, Antitumor effect of vitamin A and D on head and neck squamous cell carcinoma, *Auris Nasus Larynx* 30 (4) (2003) 403–412, 10.1016/s0385-8146(03)00091-9. [PubMed: 14656567]
- [19]. Lokman NA, Ho R, Gunasegaran K, Bonner WM, Oehler MK, Ricciardelli C, Anti-tumour effects of all-trans retinoid acid on serous ovarian cancer, *J. Exp. Clin. Cancer Res* 38 (1) (2019) 10, 10.1186/s13046-018-1017-7. [PubMed: 30621740]
- [20]. Zou C, Zhou J, Qian L, Feugang JM, Liu J, Wang X, Wu S, Ding H, Zou C, Liebert M, Grossman HB, Comparing the effect of ATRA, 4-HPR, and CD437 in bladder cancer cells, *Front Biosci.* 11 (2006) 2007–2016, 10.2741/1942. [PubMed: 16720286]

- [21]. Chaudhari N, Talwar P, Lefebvre D'hellencourt C, Ravanan P, CDDO and ATRA instigate differentiation of IMR32 human neuroblastoma cells, *Front. Mol. Neurosci* 10 (2017) 310, 10.3389/fnmol.2017.00310. [PubMed: 29018329]
- [22]. Nozaki Y, Tamaki C, Yamagata T, Sugiyama M, Ikoma S, Kinoshita K, Funauchi M, All-trans-retinoic acid suppresses interferon-gamma and tumor necrosis factor-alpha; a possible therapeutic agent for rheumatoid arthritis, *Rheumatol. Int* 26 (9) (2006) 810–817, 10.1007/s00296-005-0076-1. [PubMed: 16292516]
- [23]. Xia Q, Zhao Y, Wang J, Qiao W, Zhang D, Yin H, Xu D, Chen F, Proteomic analysis of cell cycle arrest and differentiation induction caused by ATPR, a derivative of all-trans retinoic acid, in human gastric cancer SGC-7901 cells, *Proteomics Clin. Appl* 11 (7–8) (2017), 10.1002/prca.201600099.
- [24]. Wang H, Gui SY, Chen FH, Zhou Q, Wang Y, New insights into 4-amino-2-trifluoromethyl-phenyl ester inhibition of cell growth and migration in the A549 lung adenocarcinoma cell line, *Asian Pac. J. Cancer Prev* 14 (12) (2013) 7265–7270, 10.7314/apjcp.2013.14.12.7265. [PubMed: 24460286]
- [25]. Fan TT, Cheng Y, Wang YF, Gui SY, Chen FH, Zhou Q, Wang Y, A novel all-trans retinoid acid derivative N-(3-trifluoromethyl-phenyl)-retinamide inhibits lung adenocarcinoma A549 cell migration through down-regulating expression of myosin light chain kinase, *Asian Pac. J. Cancer Prev* 15 (18) (2014) 7687–7692, 10.7314/apjcp.2014.15.18.7687. [PubMed: 25292047]
- [26]. Li G, Wang K, Li Y, Ruan J, Wang C, Qian Y, Zu S, Dai B, Meng Y, Zhou R, Ge J, Chen F, Role of eIF3a in 4-amino-2-trifluoromethyl-phenyl retinate-induced cell differentiation in human chronic myeloid leukemia K562 cells, *Gene* 683 (2019) 195–209, 10.1016/j.gene.2018.10.035. [PubMed: 30340049]
- [27]. Magaki S, Hojat SA, Wei B, So A, Yong WH, An introduction to the performance of immunohistochemistry, *Methods Mol. Biol* 1897 (2019) 289–298, 10.1007/978-1-4939-8935-5_25. [PubMed: 30539453]
- [28]. Zuo L, Lu M, Zhou Q, Wei W, Wang Y, Butyrate suppresses proliferation and migration of RKO colon cancer cells through regulating endoan expression by MAPK signaling pathway, *Food Chem. Toxicol* 62 (2013) 892–900. [PubMed: 24416777]
- [29]. Lakshmanan I, Batra SK, Protocol for apoptosis assay by flow cytometry using annexin V staining method, *Bio Protoc* 3 (6) (2013), 10.21769/bioprotoc.374.
- [30]. Kyrylkova K, Kyryachenko S, Leid M, Kioussi C, Detection of apoptosis by TUNEL assay, *Methods Mol. Biol* 887 (2012) 41–47, 10.1007/978-1-61779-860-3_5. [PubMed: 22566045]
- [31]. Yang Q, Liu Y, Huang Y, Huang D, Li Y, Wu J, Duan M, Expression of COX-2, CD44v6 and CD147 and relationship with invasion and lymph node metastasis in hypopharyngeal squamous cell carcinoma, *PLoS One* 8 (9) (2013), e71048, 10.1371/journal.pone.0071048. [PubMed: 24019861]
- [32]. Bowie GL, Caslin AW, Roland NJ, Field JK, Jones AS, Kinsella AR, Expression of the cell-cell adhesion molecule E-cadherin in squamous cell carcinoma of the head and neck, *Clin. Otolaryngol. Allied Sci* 18 (3) (1993) 196–201, 10.1111/j.1365-2273.1993.tb00829.x. [PubMed: 8365008]
- [33]. Munck-Wiki E and, Edstrom S, Jungmark E, Kuylenstierna R, Lindholm J, Auer G, Nuclear DNA content, proliferating-cell nuclear antigen (PCNA) and p53 immunostaining in predicting progression of laryngeal cancer in situ lesions, *Int. J. Cancer* 56 (1) (1994) 95–99, 10.1002/ijc.2910560117. [PubMed: 7903288]
- [34]. Tomasino RM, Daniele E, Bazan V, Morello V, Tralongo V, Nuara R, Nagar C, Salvato M, Ingria F, Restivo S, et al., Prognostic significance of cell kinetics in laryngeal squamous cell carcinoma: clinicopathological associations, *Cancer Res.* 55 (24) (1995) 6103–6108. [PubMed: 8521400]
- [35]. Shin DM, Voravud N, Ro JY, Lee JS, Hong WK, Hittelman WN, Sequential increases in proliferating cell nuclear antigen expression in head and neck tumorigenesis: a potential biomarker, *J. Natl. Cancer Inst* 85 (12) (1993) 971–978, 10.1093/jnci/85.12.971. [PubMed: 8098774]
- [36]. Tang J, Yao J, Shi J, Xiao Q, Zhou J, Chen F, Synthesis, characterization, drugloading capacity and safety of novel pH-independent amphiphilic amino acid copolymer micelles, *Pharmazie* 67 (9) (2012) 756–764. [PubMed: 23016447]

- [37]. Potier MC, Chelot E, Pekarsky Y, Gardiner K, Rossier J, Turnell WG, The human myosin light chain kinase (MLCK) from hippocampus: cloning, sequencing, expression, and localization to 3qcen-q21, *Genomics* 29 (3) (1995) 562–570, 10.1006/geno.1995.9965. [PubMed: 8575746]
- [38]. Gallagher PJ, Herring BP, Trafhy A, Sowadski J, Stull JT, A molecular mechanism for autoinhibition of myosin light chain kinases, *J. Biol. Chem* 268 (35) (1993) 26578–26582. [PubMed: 8253787]
- [39]. Van Lierop JE, Wilson DP, Davis JP, Tikunova S, Sutherland C, Walsh MP, Johnson JD, Activation of smooth muscle myosin light chain kinase by calmodulin. Role of LYS(30) and GLY(40), *J. Biol. Chem* 277 (8) (2002) 6550–6558, 10.1074/jbc.M111404200. [PubMed: 11748245]
- [40]. Turner JR, Rill BK, Carlson SL, Carnes D, Kerner R, Mrsny RJ, Madara JL, Physiological regulation of epithelial tight junctions is associated with myosin light-chain phosphorylation, *Am. J. Physiol* 273 (4 Pt 1) (1997) C1378–85. [PubMed: 9357784]
- [41]. Clayburgh DR, Rosen S, Witkowski ED, Wang F, Blair S, Dudek S, Garcia JG, Alverdy JC, Turner JR, A differentiation-dependent splice variant of myosin light chain kinase, MLCK1, regulates epithelial tight junction permeability, *J. Biol. Chem* 279 (53) (2004) 55506–55513, 10.1074/jbc.M408822200. [PubMed: 15507455]
- [42]. Cunningham KE, Turner JR, Myosin light chain kinase: pulling the strings of epithelial tight junction function, *Ann. N. Y. Acad. Sci* 1258 (2012) 34–42, 10.1111/j.1749-6632.2012.06526.x. [PubMed: 22731713]
- [43]. Yamakita Y, Yamashiro S, Matsumura F, In vivo phosphorylation of regulatory light chain of myosin II during mitosis of cultured cells, *J. Cell Biol* 124 (1-2) (1994) 129–137. [PubMed: 8294496]
- [44]. Daniel JL, Molish IR, Rigmaiden M, Stewart G, Evidence for a role of myosin phosphorylation in the initiation of the platelet shape change response, *J. Biol. Chem* 259 (15) (1984) 9826–9831. [PubMed: 6746669]
- [45]. Lazar V, Garcia JG, A single human myosin light chain kinase gene (MLCK; MYLK), *Genomics* 57 (2) (1999) 256–267, 10.1006/geno.1999.5774. [PubMed: 10198165]
- [46]. Ju J, Wang N, Wang J, Wu F, Ge J, Chen F, 4-Amino-2-trifluoromethyl-phenyl retinate inhibits proliferation, invasion, and migration of breast cancer cells by independently regulating CRABP2 and FABP5, *Drug Des. Devel. Ther* 12 (2018) 997–1008, 10.2147/DDDT.S151029.
- [47]. Zhang Y, Zhang C, Zhang H, Zeng W, Li S, Chen C, Song X, Sun J, Sun Z, Cui C, Cao X, Zheng L, Wang P, Zhao W, Zhang Z, Xu Y, Zhu M, Chen H, ZIPK mediates endothelial cell contraction through myosin light chain phosphorylation and is required for ischemic-reperfusion injury, *FASEB J.* 33 (8) (2019) 9062–9074, 10.1096/fj.201802052RRR. [PubMed: 31180722]
- [48]. Su L, Nalle SC, Shen L, Turner ES, Singh G, Breskin LA, Khramtsova EA, Khramtsova G, Tsai PY, Fu YX, Abraham C, Turner JR, TNFR2 activates MLCK-dependent tight junction dysregulation to cause apoptosis-mediated barrier loss and experimental colitis, *Gastroenterology* 145 (2) (2013) 407–415, 10.1053/j.gastro.2013.04.011. [PubMed: 23619146]

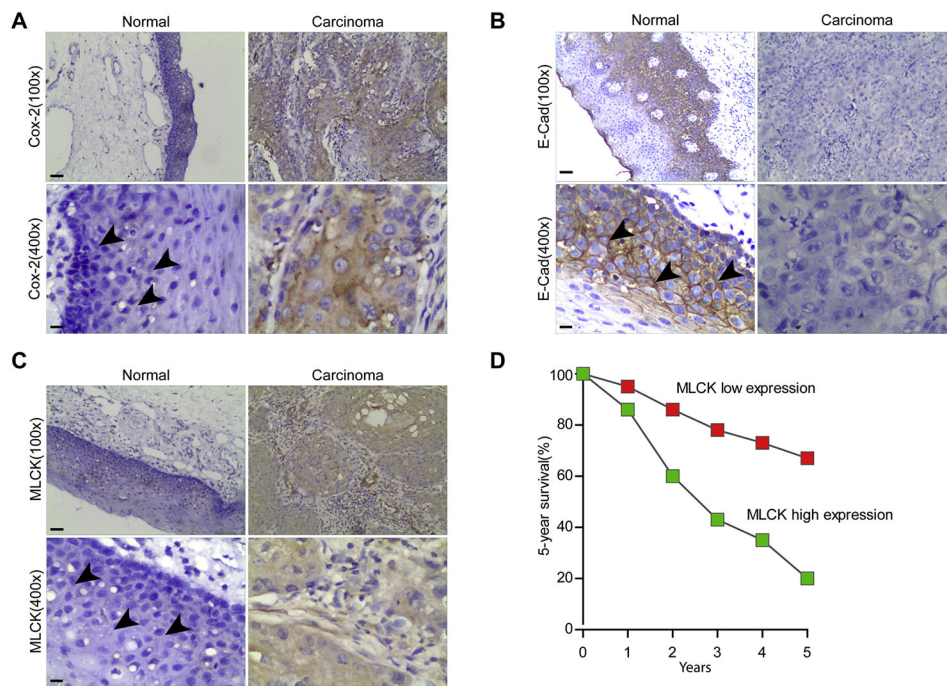


Fig. 1. MLCK is up-regulated in human hypopharyngeal carcinoma tissue and correlates with the 5-year survival rate. Expression profiles of MLCK and the markers of human hypopharyngeal cancer, including Cox-2 and E-cadherin, were analyzed. (A) Cox-2, (B) E-cadherin, and (C) MLCK expression in human hypopharyngeal carcinoma tissue were compared to adjacent non-lesion tissues. Cox-2 protein was up-regulated (A), whereas E-cadherin was down-regulated (B), demonstrating characteristics of hypopharyngeal cancer. Of interest, MLCK expression was obviously increased in hypopharyngeal carcinoma compared to adjacent healthy tissue. Bar = 50 μ m (100X, upper panel), 10 μ m (400X, lower panel), and arrows indicate the adjacent non-lesion tissues. (D) MLCK expression can be used as a prognostic marker for patients with hypopharyngeal cancer. The 5-year survival was negatively correlated with MLCK expression. The patients with low MLCK expression has higher survival rate. In contrast, the patients with high MLCK expression has low survival rate.

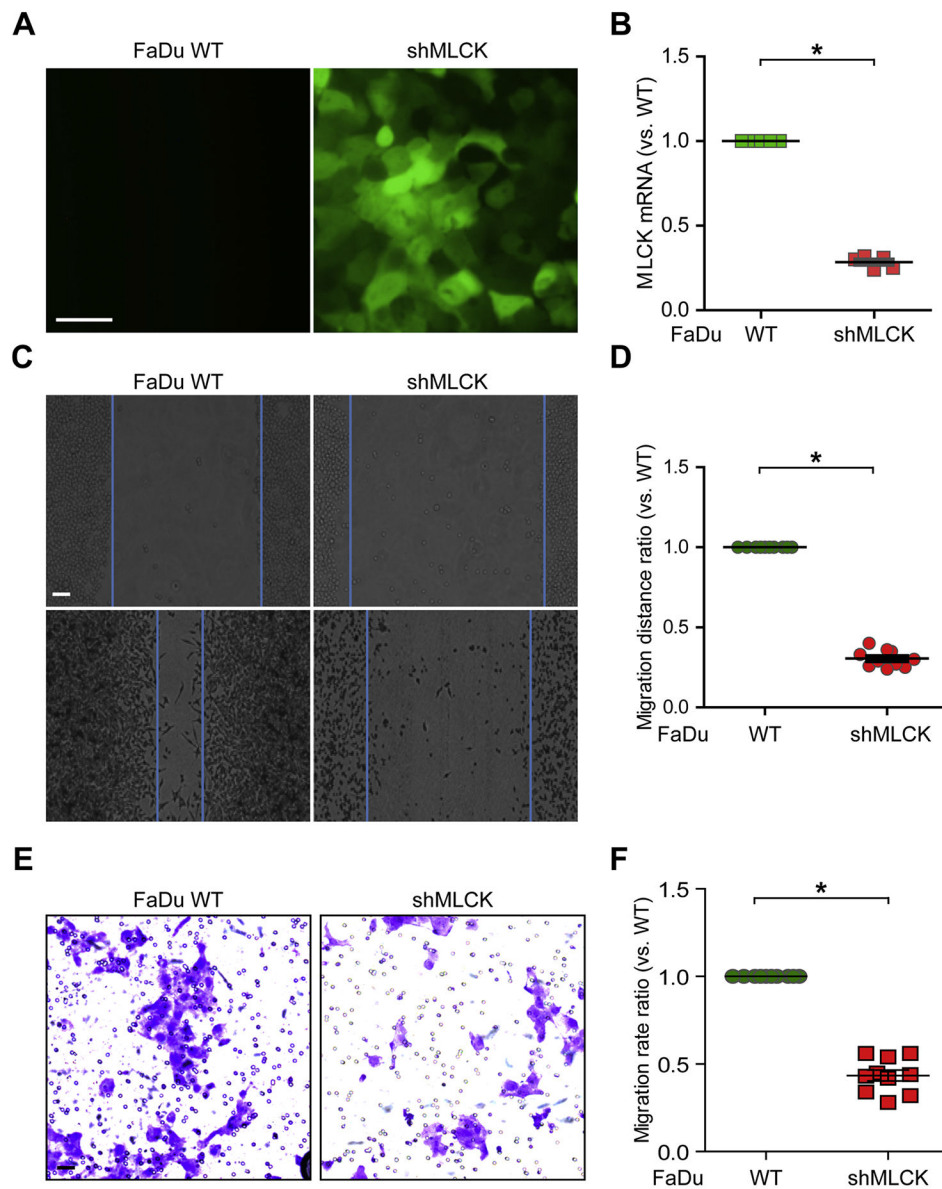


Fig. 2. MLCK expression is associated with cell migration in hypopharyngeal cancer FaDu cells. (A) GFP expression in shMLCK transfected FaDu cells confirming the transfection efficiency of shMLCK. Bar = 50 μ m. (B) MLCK transcript in MLCK knockdown cells compared to wide-type cells. The expression level of MLCK was decreased by ~70% in knockdown cells. (C) Wound healing assay showed that MLCK knockdown reduces FaDu cell migration. Bar = 50 μ m (D) The quantitative migration distance ratio of wound healing assay is around 60-70% in MLCK knockdown FaDu cells compared to wide-type cells. (E) Representative images of transwell cell migration assay indicated that migration was attenuated in MLCK knockdown FaDu cells. Bar = 50 μ m. (F) Quantitative analyses of transwell cell migration assay. Similar to the data from wound healing assay, MLCK suppression reduced cell migration ~60 - 70%. * $p < 0.05$ compared with wide-type cells.

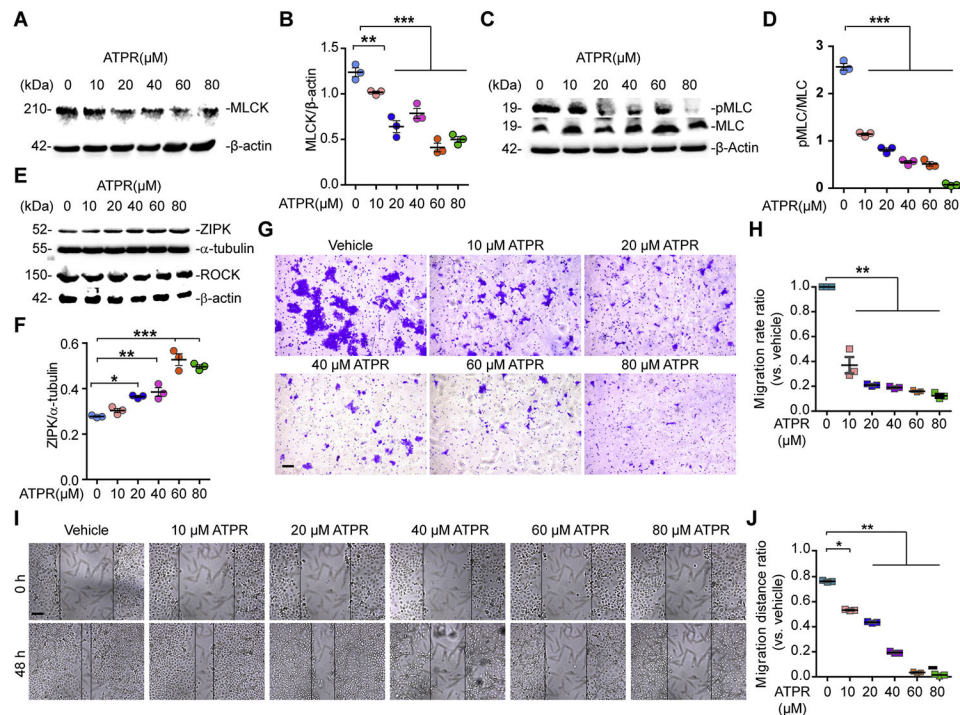


Fig. 3. ATPR reduces MLCK expression and activity in hypopharyngeal cancer cells and inhibits FaDu cell migration. (A) ATPR reduced MLCK expression in FaDu cells in a dose-dependent manner. (B) Quantification of MLCK protein level expression by Quantity one software. (C) ATPR inhibited MLC phosphorylation in FaDu cells. Since MLCK directly induced MLC phosphorylation, this data suggested that ATPR also suppressed MLCK activity. (D) Quantification of MLC phosphorylation by Quantity one software. (E) Effects of ATPR on ZIPK and ROCK expression in FaDu cells. ZIPK and ROCK have been considered as the other regulators of MLC phosphorylation. We therefore analyzed the expression of these two proteins. Although ATPR did not decrease ROCK expression, it dose-dependently increases ZIPK expression. (F) Quantification of ZIPK protein level expression in FaDu cells by Quantity one software. (G-J) Transwell cell migration and wound healing assays showed that ATPR significantly inhibited cell migration in a dose-dependent manner. Bar = 50 μm . * $p < 0.05$; ** $p < 0.01$ compared with vehicle control.

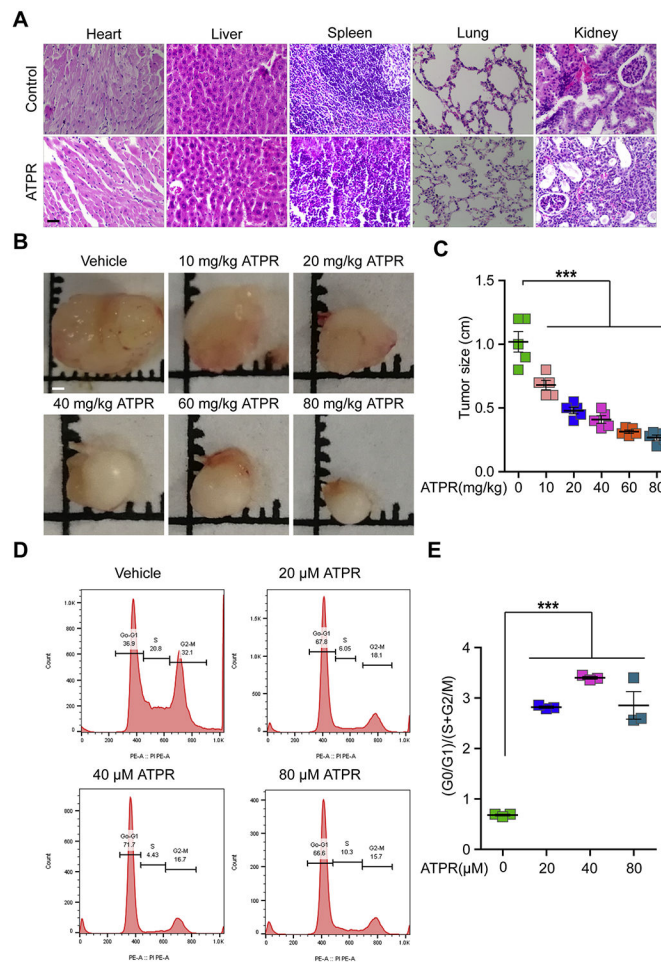


Fig. 4. ATPR is non-toxic and effective for hypopharyngeal cancer treatment. (A) H&E staining of mouse tissues, including heart, liver, spleen, lung, and kidney, compared to control mice, ATPR treatment did not induce morphologic abnormalities in these vital organs. This result suggested that ATPR is non-toxic at this dose *in vivo*. Bar = 50 μm. (B) To generate a xenograft mouse model of hypopharyngeal cancer, mice were subcutaneously injected with 10^7 FaDu cells. Tumor size was measured after 6 weeks post-injection, ATPR reduced tumor growth in nude mice in a dose-dependent manner. Bar = 1 mm. (C) Quantification of the effect of ATPR on tumor size in mice, five mice per group. (D) Flow cytometry was performed to detect the effects of ATPR in FaDu cell proliferation. (E) Quantitative analysis of flow cytometry. ATPR induced cell cycle arrest at the G0/G1 phase in FaDu cells. *** p < 0.001 compared with vehicle control.

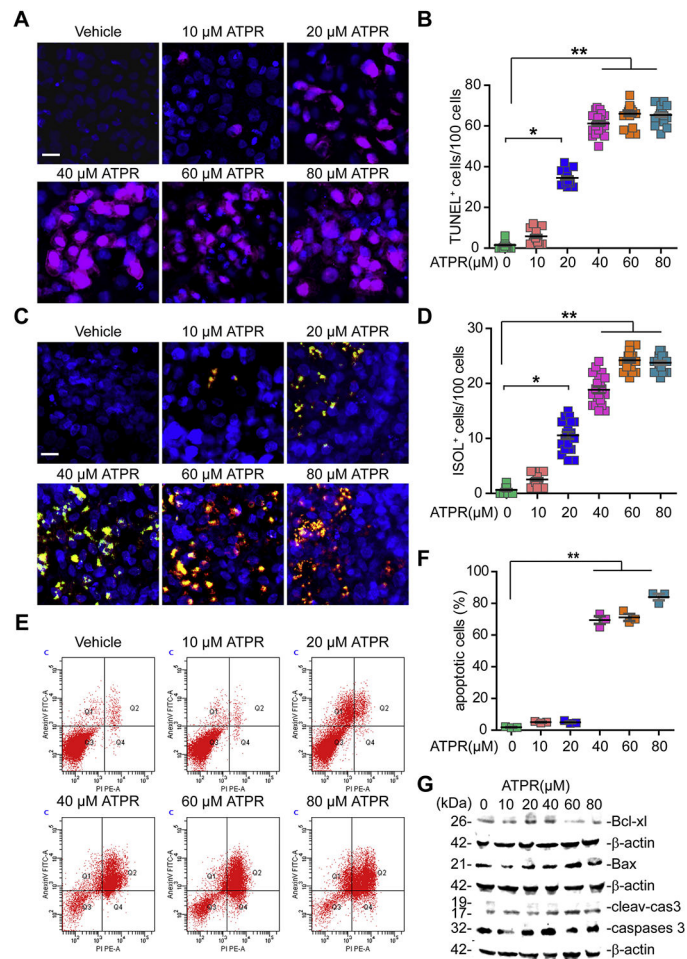


Fig. 5. ATPR induces hypopharyngeal cancer cell apoptosis. (A) Representative TUNEL staining in FaDu cells treated with or without ATPR. Bar = 20 μm . (B) Quantification of TUNEL staining. (C) ISOL staining was performed in FaDu cells treated with or without ATPR treatment. Bar = 20 μm . (D) Quantification of apoptotic cells in ISOL staining. (E) Flow cytometry analysis of cell apoptosis in ATPR-treated group compared to vehicle control FaDu cells. (F) Quantification of apoptotic cell ratio in flow cytometry assay. Based on TUNEL, ISOL, and flow cytometry assays, ATPR promoted apoptosis in FaDu cells in a dose-dependent manner. (G) Immunoblots of apoptotic associated protein signals in FaDu cells treated with or without ATPR. Importantly, ATPR increases expression of pro-apoptotic protein, including cleaved caspase-3 and Bax, in parallel with suppressing anti-apoptotic protein Bcl-xl. * $p < 0.05$; ** $p < 0.01$ compared with vehicle control.

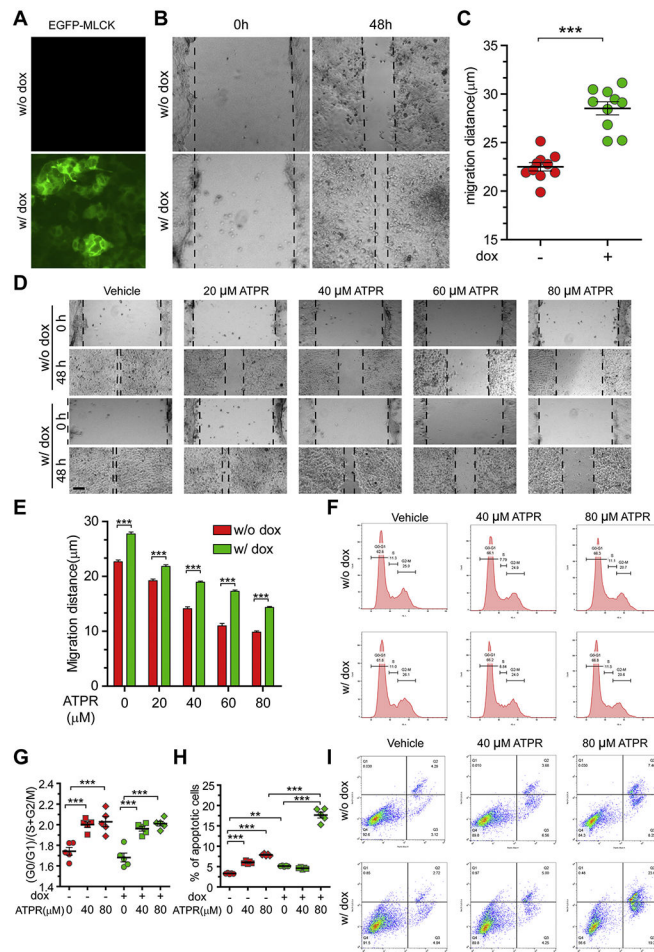


Fig. 6. Anti-cancer activities of ATPR on MLCK-overexpressing FaDu cells. (A) EGFP-MLCK expression induced by doxycycline (dox) treatment in FaDu cells transfected with pPBH-TREtight-EGFP plasmid. Bar = 20 μm . (B, C-) Wound healing assay revealed that, in inducible EGFP-MLCK overexpressing FaDu cells, the migration rate was increased. *** $p < 0.001$ compared with w/o dox. (D-E) Effect of ATPR on cancer cell migration inhibition was attenuated in EGFP-MLCK overexpressing FaDu cells. Bar = 50 μm . *** $p < 0.001$ compared with w/o dox. (F-) ATPR induced cell cycle arrest at G0/G1 phase in dox-treated and untreated EGFP-MLCK overexpressing FaDu cells. *** $p < 0.001$ compared with vehicle control. There is no difference between dox treatment and without dox group. (H, -I) Effect of ATPR-induced cancer cell apoptosis was potentiated in EGFP-MLCK overexpressing FaDu cells. *** $p < 0.001$ compared with w/o dox or vehicle.

Table 1

shRNA of MLCK

ID	Target Sequence	Start Position
NT	CAACAAGATGAAGAGCACCAA	
1#	GACGGGAAGTCTCTTTAA	5866
2#	GCGGGAAGGATTCTTCAA	94
3#	GTGCATGTGTGGCGTATAT	7672

Author Manuscript

Author Manuscript

Author Manuscript

Author Manuscript

Table 2

The relationship between MLCK expression and pathological parameters

Pathological parameters	N	MLCK expression		P Value
		-/+	+/+++	
Sex				
Male	104	47	57	>0.05
Female	4	2	2	
Age				
≥60	68	30	38	>0.05
<60	40	19	21	
Tumor size(cm)				
T1	14	6	8	>0.05
T2	50	23	27	
T3	22	10	12	
T4	22	10	12	
Tumor metastasis				
N0	0			<0.05
N1	38	20	18	
N2	68	29	39	
N3	2		2	